

Copyright Notice:

©2005 IEEE. Personal use of this material is permitted. However, permission to reprint/republish this material for advertising or promotional purposes or for creating new collective works for resale or redistribution to servers or lists, or to reuse any copyrighted component of this work in other works must be obtained from the IEEE.

Broadband/Multiband Conformal Circular Beam-Steering Array

Johnson J. H. Wang, *Life Fellow, IEEE*, David J. Triplett, and Chris J. Stevens, *Member, IEEE*

Abstract— A new approach for a broadband/multiband conformal circular beam-steering array is presented with both theory and experimental data. The array is low-profile, suitable for conformal mounting on a platform. It has an omnidirectional coverage with a unidirectional beam that aims at a moderate antenna gain of 5 to 15 dBi. It consists of a center driven element and parasitic surface waveguide elements symmetrically positioned in the periphery for electronic beam steering. This array can achieve ultra-wideband multiband performance and low-profile conformability unattainable by conventional array approaches. In addition, its cost is estimated to be an order of magnitude lower than that of conventional beam-steering arrays. Breadboard and brassboard development efforts for the array have essentially achieved a bandwidth of 1.0–2.5 GHz. A larger bandwidth is feasible since its driven element has achieved a continuous 10:1 bandwidth, and since the surface waveguide elements could achieve a multi-octave bandwidth similar to the broadbanding effort from the Yagi-Uda array to the LP array.

Index Terms— Arrays, beam steering, circular arrays, conformal antennas, multi-frequency antennas.

I. INTRODUCTION

THERE is a growing need for broadband/multiband beam-steering antennas driven by applications such as the software radio and WLAN (Wireless Local Area Network), among others. In these applications, steerable beams with an antenna gain of 5–15 dBi and omnidirectional coverage in the azimuth plane are generally desired. It is also needed that the antenna be broadband/multiband, covering 1–2.5 GHz or more. For practical applications, they must meet demanding conformability requirements for mounting on a moving platform. As such, they must have a low profile and be suitable for mounting on certain limited locations, such as the top or bottom surface, on the platform. Furthermore, cost is generally a major consideration.

Beam-steering arrays can be generally classified as: (1) phased arrays, (2) switched-element arrays, and (3) parasitic arrays. Existing antenna arrays are mostly of the phased or switched-element types. Unfortunately, these two types are

expensive, bulky, and complex; though extensively researched, few of them have been deployed.

The third type, the parasitic array, but without beam steering, is widely used mainly due to their low cost. To achieve beam steering, a circular beam-steering parasitic array had been originally patented by Yagi [1], and its low-cost merits have been recognized and explored by many (e.g., [2]). However, to date they are invariably narrowband, typically employing monopole antennas as the driven and parasitic array elements. In addition, they have a high profile resulting from the use of resonant monopoles for both driven and parasitic elements.

This paper presents a beam-steering array antenna of the third type, the circular parasitic array evolved from the initial concept of Yagi [1] but significantly revolutionized to achieve broadband/multiband and low-profile. The approach is based on a patent-pending technique [3], with some results presented recently in [4]. This paper presents a fairly complete discussion on the design approach, the theory, experimental data, as well as the practical applications and merits of this new beam-steering array design.

II. BROADBAND LOW-PROFILE CIRCULAR TRAVELING-WAVE (TW) BEAM-STEERING ARRAY

Fig. 1 shows the top and side views of the circular beam-steering array with a height of h_λ and diameter of D_λ , where λ is the wavelength at the lowest operating frequency.

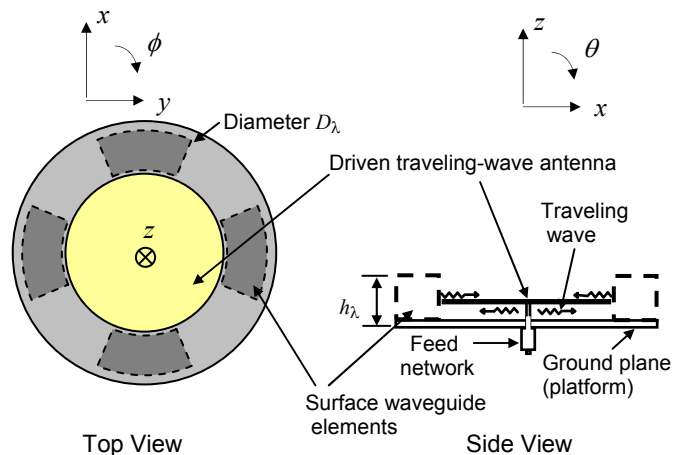


Fig. 1. Broadband/multiband beam-steering circular traveling-wave array.

Manuscript received March 31, 2005. This work was supported in part by the U.S. Army SBIR program under Contract W15P7T-04-C-L403 sponsored by U.S. Army CECOM, Ft. Monmouth, NJ.

The authors are with Wang Electro-Opto Corporation, Marietta, GA 30067 USA. (phone: 770-955-9311; fax: 770-984-9045; e-mail: jjhwang@weo.com).

The array is conformally mounted on the top or bottom surface (conducting ground plane) of a platform to generate a directional beam electronically steered in the x - y plane for 360° omnidirectional azimuth coverage. The array is a small, low-profile (one to two inches high) circular traveling wave (TW) array expected to achieve a 2.5:1 bandwidth (1-2.5 GHz). But, D_λ must be large enough to accommodate the radiation zones, to be discussed in III-B, for effective radiation.

The array consists of a single driven element antenna in the center and multiple electronically controlled surface waveguide elements that are concentrically and symmetrically positioned around the driven element. The center driven element, a broadband/multiband omnidirectional traveling-wave antenna, is connected via a feed line to the receiver and/or transmitter.

Without loss of generality, the theory of operation can be explained by considering the transmit case; the receive case is similar in light of reciprocity. In Fig. 1, a traveling wave is emitted from the center of the driven traveling wave element antenna and propagates along, and intimately bound to, the ground plane as well as the traveling wave structure.

The surface waveguide elements shown in Fig. 1 are variable filters which pass or reflect the incoming traveling wave. The filtering action is governed by control circuits, not shown in Fig. 1, which control the impedance state of each surface waveguide element. Each surface waveguide element presents two possible states to the traveling wave, to pass or reflect the incoming traveling wave as a filter, thus generating a steerable beam. The simplicity of this array design leads to a tremendous low-cost advantage.

Analogous to the enormous success in broadbanding linear Yagi-Uda arrays over the last eight decades, ultra-wideband performance of the present circular parasitic array can be achieved by designing the array as a traveling wave (TW) structure with broadband driven and parasitic elements.

III. THE DRIVEN CENTER ELEMENT OF THE ARRAY

A. The Ultra-wideband Traveling Wave (TW) Antenna

The driven antenna in the center of the array in Fig. 1 is an ultra-wideband omnidirectional traveling-wave (TW) antenna, as depicted in Fig. 2.

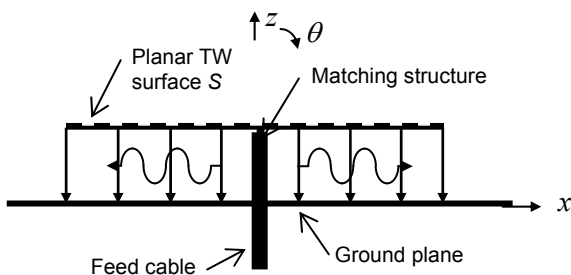


Figure 2. The center driven traveling-wave (TW) antenna.

Both mode-0 SMM (spiral-mode microstrip) antennas [5], [6] and mode-0 slow-wave antennas [7] have been used in this design. For the convenience of the present discussion, we will focus on the design based on the SMM antenna, which has a low profile and an ultra-wideband omnidirectional pattern bandwidth amply suitable for the present application.

The mode-0 spiral is the case in which all the spiral arms are excited with the same phase and amplitude. It is assumed here that the planar structure S is self-complementary, in this case a self-complementary multi-arm spiral. It is also assumed that a TW has been successfully launched and maintained; under this assumption the equivalent surface currents can be readily derived from a simple TW theory in closed form since the source and fields are sufficiently decoupled. Approximate antenna properties, including gain pattern and impedance, can be obtained under these assumptions.

The multi-arm spiral planar TW surface is equivalent to an array of concentric annular slots. Thus, the antenna's radiated fields are the superposition of the contributing fields from these concentric annular slots along ρ and a circular slot at the edge of S . This relationship is both physically and mathematically significant, and we will take advantage of this relevance by examining the annular slot first.

B. The Mode-0 SMM Antenna as an Array of Concentric Annular Slots Plus Edge Slot

To treat the mode-0 SMM antenna as an array of concentric circular annular slots, plus a circular slot at the rim of S , we will first formulate the problem for the circular annular slot *per se* as depicted in Fig. 3. For the convenience of this discussion, the annular slot is assumed to be on the x - y plane, with a radius a at the center line of the slot. The slot, of width δ , is excited by a uniform radial electric field E parallel to the ρ axis of the cylindrical coordinate system, with a resulting voltage V ($V = \delta E$) across the slot aperture.

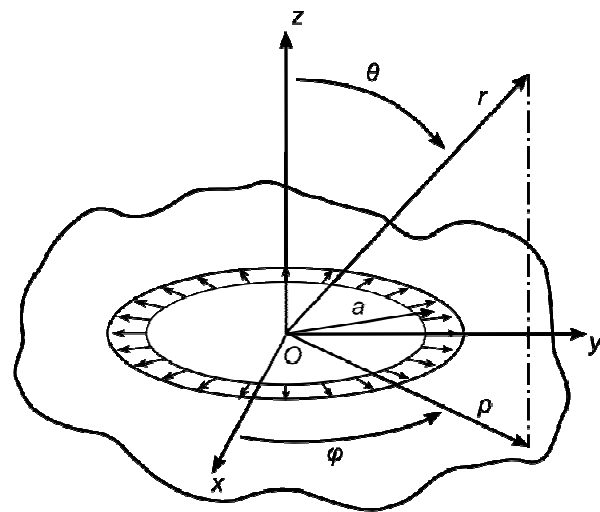


Fig. 3. An annular slot on x - y plane.

It can be shown that the far-zone radiation of a thin (small δ/λ) annular slot is fully represented by a magnetic field having only a ϕ component, as follows:

$$H_\phi(\phi) = \frac{jaV \exp(-jkr)}{120\pi\lambda r} \int_0^{2\pi} \cos(\phi - \phi') \exp[jka \sin\theta \cos(\phi - \phi')] d\phi' \quad (1)$$

where the primed and unprimed coordinates refer to the source and field points, \mathbf{r} and \mathbf{r}' , respectively; $r = |\mathbf{r} - \mathbf{r}'|$; and the $e^{j\omega t}$ convention is taken. The integral in Eq. (1) can be evaluated exactly, yielding

$$H_\phi = \frac{-aV \exp(-jkr)}{60\lambda r} J_1(ka \sin\theta) \quad (2)$$

where J_1 denotes a Bessel function of the first kind of order 1.

For a slot of a small diameter ($a \leq \lambda/(2\pi)$), Eq. (2) can be approximated by

$$H_\phi \cong \frac{-V \exp(-jkr)}{60r} \frac{A}{\lambda^2} \sin\theta \quad (3)$$

where $A = \pi a^2$.

Although the theory for far-zone radiated fields of a thin circular annular slot with uniform aperture excitation have been known for over half a century, they have been formally reported, to the best of our knowledge, only in the antenna handbook [8], [9] and the original paper [10]. Unfortunately, the results in both references, in the form of Eqs. (1)-(3), have some errors. Although the senior author plans to present the corrected equations and their derivation in a symposium, it is desirable to formally publish the key equations here and to facilitate the present discussion.

It is worth pointing out that Eqs. (2) and (3) can be verified independently by invoking duality from the case of a circular electric loop antenna based on Maxwell's equations having full-fledged presentation of magnetic sources [11].

The far-zone radiated magnetic field of the mode-0 SMM antenna, as an array of concentric annular slots, consists of a ϕ component only and is given by

$$H = H_\phi = \sum_{\ell=1}^{\ell=N} H_\ell(\theta, \phi) = \sum_{\ell=1}^{\ell=N} \frac{-a_\ell V_\ell \exp(-jkr)}{60\lambda r} J_1(ka_\ell \sin\theta) e^{j\psi_\ell} \quad (4)$$

where ψ_ℓ and V_ℓ denote, respectively, the phase and amplitude of the voltage of annular slot element ℓ located at a radial distance $\rho = a_\ell$.

The series in Eq. (4) can be approximately evaluated by the method of stationary phase by including only a few terms with in-phase contribution. Physically, this means including only annular slots in the "radiation zones." For a 2-arm mode-0

spiral, the radiation zones are at circumferences where the phase change $\Delta\psi_\ell$ equals $\pi/2$ between adjacent arms so that an equivalent annular slot is formed over two rings of adjacent annular slots, with a resulting voltage V across it. For a 4-arm mode-0 spiral, $\Delta\psi_\ell = \pi/4$ between adjacent arms at the radiation zone; four adjacent slots are needed to form an equivalent annular slot. Thus, the radiation zones are at circumferential rings with radii ρ_r given by

$$\rho_r = \lambda/(4\pi) + n\lambda/\pi \quad \text{for 2-arm spiral} \quad (5a)$$

$$\rho_r = \lambda/(8\pi) + n\lambda/\pi \quad \text{for 4-arm spiral} \quad (5b)$$

where $n = 0, 1, 2, 3, \dots$

It is noteworthy that the present theory is in closed form, thus readily provides physical insights without the need for numerical analysis that often clouds the physics involved. As a result, the design optimization process can be carried out efficiently. Later we will present some computed data and compare them with the theory.

C. Impedance Matching for the TW Antenna

The planar TW surface S can be considered a loaded surface consisting of both a reactive component and a resistive component, the latter accounting for possible radiation through the nonconducting (slot) region. At the rim of S , a circular slot radiates the residual power as discussed in the preceding subsection.

In regions where the planar structure S is a solid conductor, the TW structure can be viewed as a circular radial waveguide of height h , with its characteristic impedance Z_{00} at ρ for the $m = n = 0$ mode given by

$$Z_{00} = 60h/\rho \quad (6)$$

Note that Z_{00} changes with the distance from the center of the radial waveguide, yet is independent of frequency.

In regions where S is self-complementary and higher-order modes are suppressed, the characteristic impedance Z_c is

$$Z_c \sim 2 Z_{00} \quad (7)$$

Eq. (7) is based on the self-complementary geometry of the planar TW surface S and the principle of duality inherent in Maxwell equations having full-fledged presentation of magnetic sources [11].

Eqs. (6) and (7) are consistent with our empirical observations. They provide the basis for ultra-wideband impedance matching under the condition that higher-order modes are suppressed. Indeed, excellent impedance matching over a 10:1 bandwidth (1-10 GHz) has been achieved, with $\text{SWR} < 1.3$ mostly, rising to < 2.0 only at high and low frequencies, as has been presented in a symposium paper in [1].

D. Gain Pattern Performance of the Center Driven Element

Several mode-0 SMM antenna breadboard models, each about 5.7-inch in diameter and 1.06-inch in height, mounted

on a conducting ground plane of 1-ft diameter, were designed, fabricated, and tested successfully.

Fig. 4 exemplifies a comparison between computed and measured elevation radiation patterns, carried over 0.5-10.0 GHz. As can be seen, the agreement between theory and measured data is very good at the lower frequencies, but gradually deteriorates as the frequency increases. Obviously, the theoretical model which assumes no higher-order modes deviates more and more from reality as the frequency increases. In fact, at 10 GHz the height of the radial waveguide is about 1 free-space wavelength, the traveling wave can no longer be tightly bound to the microstrip-line mode, and the radiation of the edge at the rim of S becomes significant.

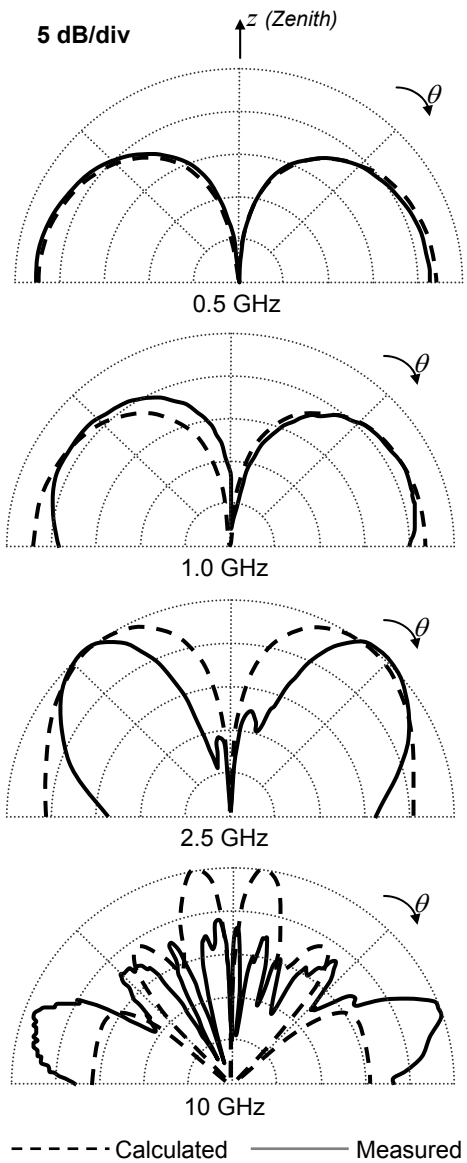


Fig. 4. Comparison between computed and measured elevation radiation patterns.

Fig. 5 shows the measured gain (at the beam peak) of the mode-0 SMM antenna over the frequency range of 0.5–10

GHz. As can be seen, the antenna has a 10:1 gain bandwidth (over 1.0-10 GHz) with a minimum gain of 1 dBi. The measurement was conducted at WEO’s anechoic chamber and calibrated against standard gain antennas. This antenna has also been measured by an Army laboratory, which confirmed the results within the operating frequency range of its antenna test facilities.

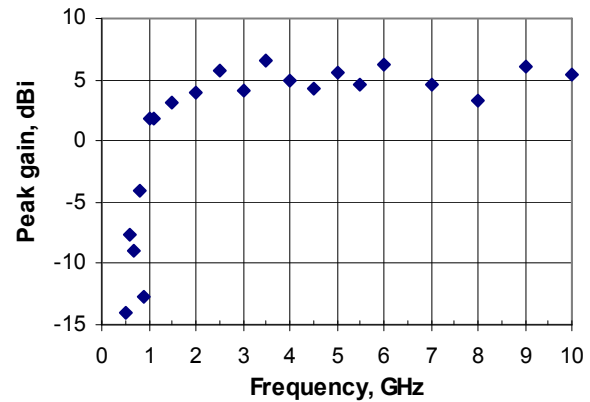


Fig. 5. Measured gain of mode-0 SMM antenna.

IV. PARASITIC SURFACE WAVEGUIDE ELEMENTS

In order to achieve beam-steering over the desired frequency range, surface waveguide elements employed in this array must function, over broad frequency bands, as either a passband filter or a band reject filter depending on their individual switching states. This concept is different from the resonant director and reflector functions that the parasitic elements perform in the Yagi array [1], [2]. That broadband surface waveguides, instead of conventional resonant parasitic elements, are used here is a foundation for the broadband/multiband performance of this circular array.

The passive array elements surrounding the center driven element act as variable filters which pass or reflect the incoming traveling wave. The filtering states of the passive elements are governed by a control circuit, thus providing electronic steering of the array. These surface waveguides are filters made of distributed elements, versus filters made of lumped elements at lower frequencies, and are a section of the transmission line supporting the traveling wave.

The broadband/multiband feature of these surface waveguides is rooted in the physics of the surface wave which can be supported on a generally planar and preferably reactive surface. Fig. 6 shows a surface waveguide consisting of a set of conducting plates, rods, or a corrugated structure above a conducting surface.

A surface wave is also supported on a purely conducting and essentially planar surface. The surface waveguide can support a surface wave with no low-frequency cutoff, and has only a minimal number of discrete modes. The selection of the surface waveguide must be based on the traveling wave that propagates in the TW structure.

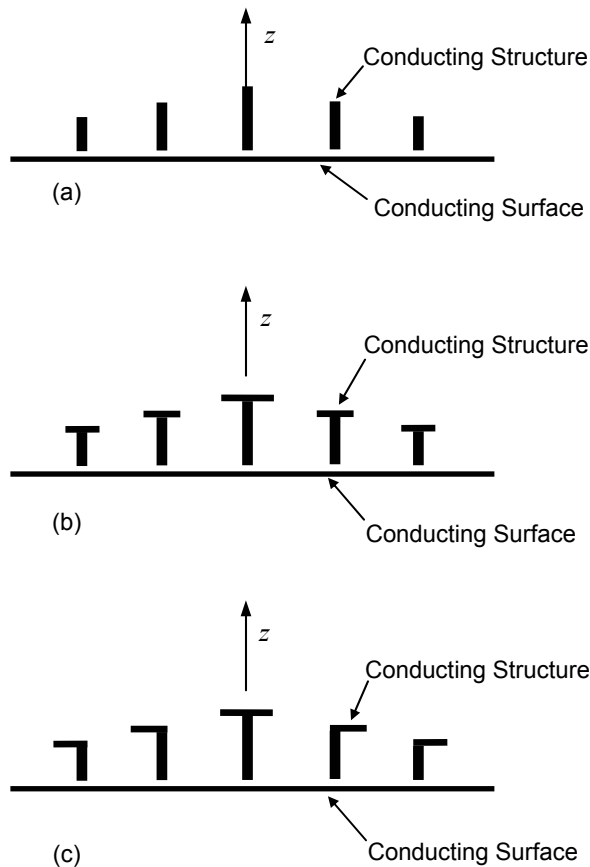


Fig. 6. Surface waveguides consisting of a set of conducting plates, rods, or a corrugated structure above a conducting surface.

The transverse magnetic mode has electric fields perpendicular to the plane surface and in the direction of propagation. The corrugated surface is a well known surface waveguide for the transverse magnetic surface wave. Equally important is that it can either pass or reject the surface wave.

Although there are many surface wave guides, for the present application only those with variable filtering actions controllable electronically are potential candidates. Thus, the surface waveguide in Fig. 6 has binary states achieved by shorting or opening the small gap with a device such as a PIN diode, resulting in a connection or disconnection between the corrugated structure and the conducting surface.

Theory for the surface waveguides in Fig. 6 predicts broadband filtering action in both states. The filtering bandwidth of a given surface waveguide element can be expanded by the use of frequency-independent structures. For example, it can be derived from a periodic structure or a log-periodic (LP) structure. Using this technique, each surface waveguide element is a log-periodic structure with its impedance state controlled as a single unit.

There are various LP structures. For the present application, only those that are amenable to switching of their impedance states are selected for experimentation. These closely related LP structures include, but are not limited to, the zigzag

antennas, the LP dipole arrays, etc.

A simple implementation is similar to that of the LP dipole array, for which the basic theory has been well established. The data for the LP dipole array can be applied to the case of the LP monopole array and used as a basis for the surface waveguide elements. This approach has the advantage of convenience in implementing control circuits for the switching of impedance states.

The broadbanding potential of such surface waveguide structures is readily envisioned in light of the historical perspective that the bandwidth of the Yagi-Uda array has expanded from about 1% in its early stage to perhaps 2000% in the form of log-periodic arrays.

V. ELECTRONIC SWITCHING OF SURFACE WAVEGUIDE ELEMENTS

As has been discussed earlier, each surface waveguide element has two distinct impedance states. In the first state, the surface waveguide element is shorted to the ground plane, and in the second state it is isolated from the ground plane. For ideal beam-steering the two states should represent absolute “short-circuit” and “open-circuit” conditions.

In practice, the connection or isolation from the ground plane is accomplished by an electronically-controlled switching circuit. One such practical circuit uses PIN diodes for the RF switching, and a lumped-element low-pass filter on the DC control line which biases the PIN diodes. It is essential that the circuit adequately isolates the RF energy from transfer to the control circuitry in order to maximize the effective gain of the antenna system.

A breadboard switching circuit using PIN diodes has been successfully designed, fabricated, and tested to demonstrate the feasibility of the approach. Over the 1-2.5 GHz range, the switching circuit has achieved isolation of > 20 dB between the surface waveguide element (located above the antenna ground plane) and the control circuit (located behind the antenna ground plane).

For better RF isolation, photovoltaic Field-Effect Transistor (PV-FET) switches are probably more suitable [12]. Optically coupled control of PV-FET switches can offer a significant increase in the isolation between the RF and control circuits, and therefore improve the performance of the array system. The broadband nature of such FET switches has been previously demonstrated.

VI. BEAM-STEERING MECHANISMS FOR THE CIRCULAR TRAVELING-WAVE ARRAY

Fig. 7 shows the block diagram for the beam-steering array for installation on a moving platform in a WLAN application. The array is a “smart antenna” that directs its beam toward another transceiver in the WLAN system under a beam-steering command. The command can be based on a signal from the targeted transceiver, or from an internally programmed input from local embedded geolocator.

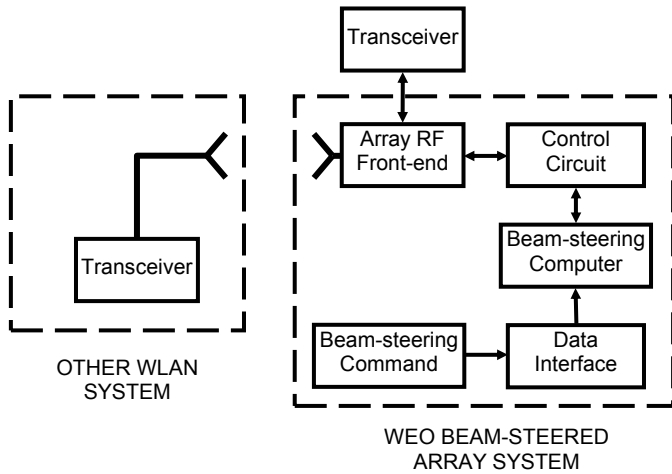


Fig. 7. System block diagram.

A number of mature approaches and algorithms for beam steering in conventional phased arrays and switched-beam arrays already exist. However, since the parasitic array has a single RF port, most conventional beam-steering algorithms are inadequate for it. Thus, a significant amount of research has been devoted in recent years to development of beam-steering algorithms for use in parasitic arrays [2].

The immediate application for the present design is on a moving platform for broadband wireless networking. There are several approaches to establish a communications link. In one approach, the array system determines the required beam-steered radiation pattern based on the positions of each node of the network. The relative positions are determined from its internal geolocation sensors embedded in each array system.

The array system uses embedded Global Positioning

System (GPS) and Inertial Navigation System (INS) sensors to determine the position and attitude of the platform and the array. The beam-steering computer for a given array system uses the position and attitude data for that array along with the position of a remote array to calculate the desired beam direction. The position of each remote array is transmitted over the wireless LAN to nearby network nodes, allowing the array system to maintain a directional link between multiple moving platforms.

VII. BREADBOARD DEVELOPMENT EFFORT

The preceding sections presented the design of an ultra-wideband/multiband circular array system as well as the enabling technologies necessary for the design approach. Breadboard and brassboard development efforts to demonstrate the full 1–2.5 GHz beam-steered array have been pursued in a “spiral” manner, and have shown promising results. The center driven traveling-wave antenna has been well developed, as discussed earlier. Development for the beam-steering computer, the control circuit, the beam-steering command, and its data interface has been largely successful, resulting in their functionality, physical compatibility, and low-cost feature fairly well established. The broadband matching of the surface waveguide remains as the only technical difficulty.

Breadboard models have achieved a beam-steering bandwidth of 1.0–2.5 GHz except for two or three narrow bands of low performance, mainly limited by the bandwidth of the surface waveguide. Fig. 8 shows measured azimuth radiation patterns with a directive beam toward $\phi = 0$, over 1.0-2.5 GHz.

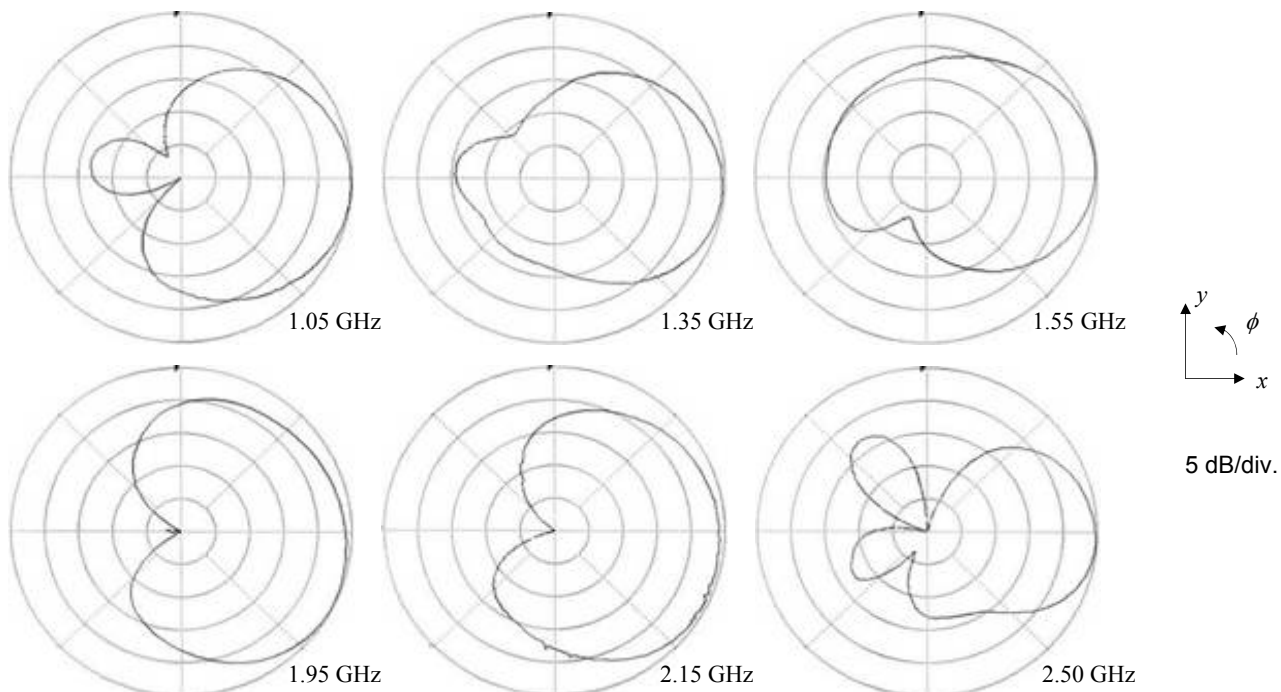


Fig. 8. Measured azimuth radiation patterns of breadboard array mounted on a 24-inch diameter ground plane.

Fig. 9 shows measured elevation patterns with a directive beam toward $\theta = 90^\circ$ over 1.0-2.5 GHz. Although there is an undesirable, yet generally unavoidable, beam tilt of 30° to 45° , the desired coverage over the 1–2.5 GHz bandwidth is essentially achieved. The beam-steering feature of the array is

exemplified by the measured azimuth radiation patterns for eight steered beams, covering full azimuth angles over 360° , at a selected frequency, as shown in Fig. 10.

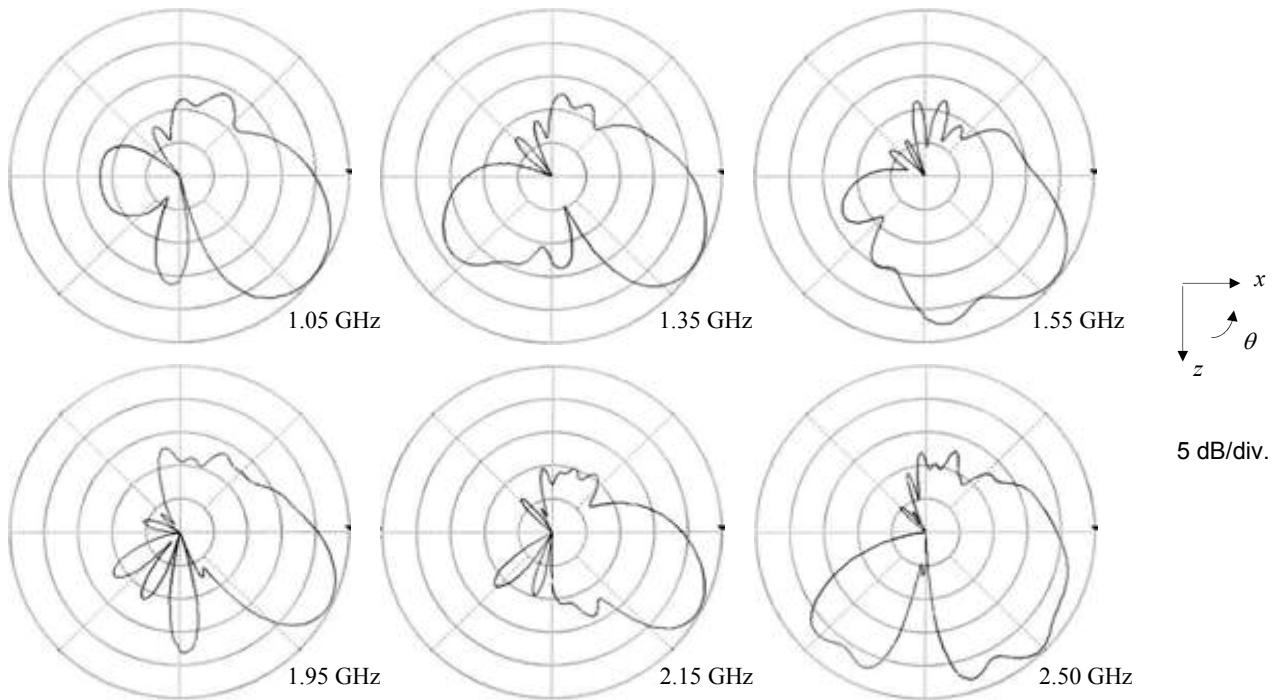


Fig. 9. Measured elevation radiation patterns of breadboard array mounted on a 24-inch diameter ground plane.

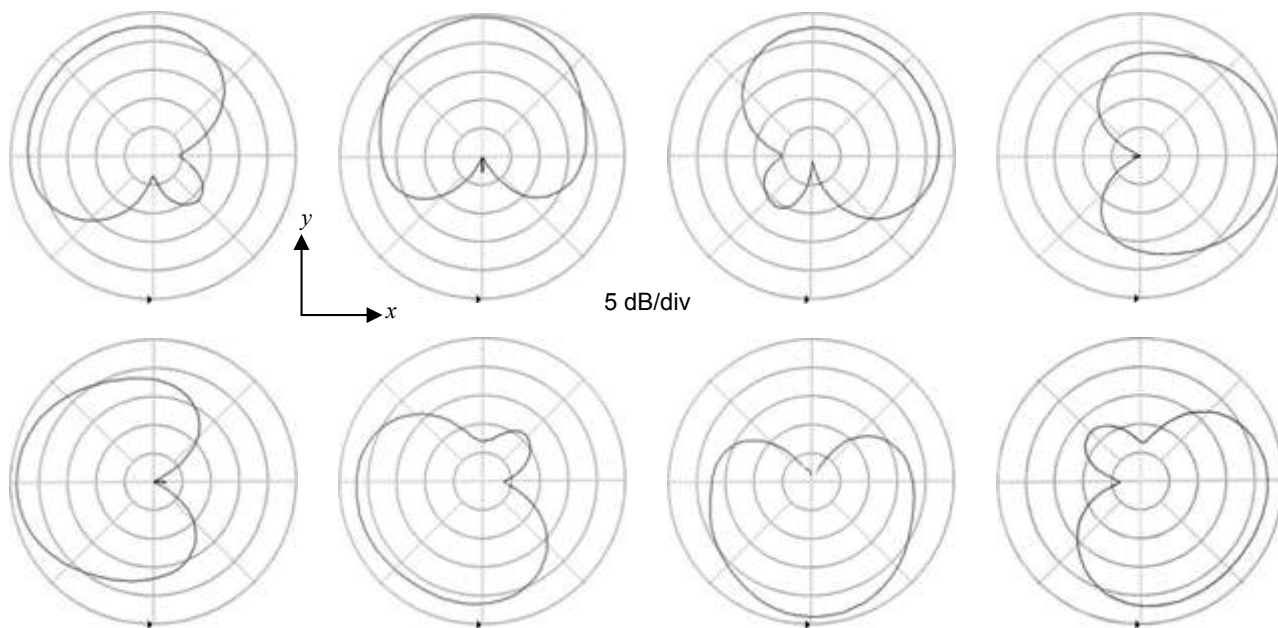


Fig. 10. Measured azimuth radiation pattern at a selected frequency, showing beam steering covering full azimuth angle of 360° .

The display panel of a beam-steering computer (BSC), including both hardware and software, developed in this research is shown in Fig. 11. The array has a manual mode and an automatic mode. The display panel of the BSC shows several key features of the beam steering in real time, which are useful for the operator as well as the engineer at this development stage.

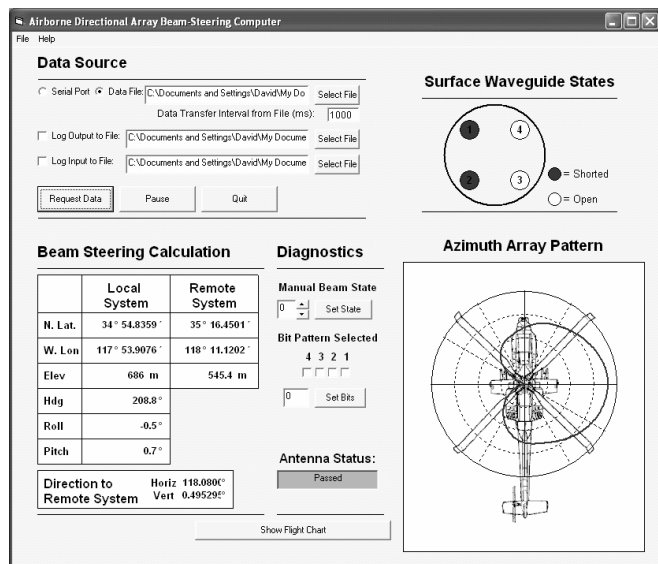


Fig. 11. Screen capture of display panel of beam-steering computer.

VIII. SIZE, SHAPE, WEIGHT, CONFORMABILITY, COST, ETC.

As discussed in the introduction section, this beam-steering array antenna is aimed at practical applications on moving platforms. Therefore, in addition to broadband/multiband performance, it must be small, low-profile, light-weight, and rugged, suitable for mounting on ground and airborne vehicles. Earlier research at Wang Electro-Opto Corporation using conventional phased array and switched-element array techniques had encountered severe difficulties in meeting these requirements. Perhaps more significantly, conventional approaches are much more costly and complex than the present approach.

A cursory analysis has been performed to assess the production cost of this array. While necessarily depending on the quantities involved, the production cost for this array antenna is roughly one order of magnitude lower than that for conventional phased arrays.

The high cost of conventional phased arrays is mainly due to the fact that they perform beam forming at the array elements, which are at the expensive RF level. The resulting complexity and per-module cost in conventional broadband/multiband electronically steered phased arrays are of course well known. As a result, conventional beam-steering phased arrays have been designed only for military and space applications, which are less sensitive to cost pressure.

In the present design of parasitic array, the switching is performed at frequencies one to two orders of magnitude

lower than the RF operating frequencies. At these low frequencies, switching circuits benefit from low-cost commercial-off-the-shelf parts and are thus extremely inexpensive.

Fig. 12 shows a photograph for a brassboard model of the entire circular beam-steering array, protected by a radome, with its beam-steering computer excluded from the photo, in contrast of a regular ballpoint pen 5.5-inch long. (All the control circuits, data interface, etc. are contained in a thin, small-diameter, multi-layer PC board underneath the aluminum mounting plate with 8 mounting holes.) As can be seen, its small size and low-profile shape are attractive in comparison with other electronic beam-steering arrays.



Fig. 12. A brassboard model of the circular beam-steering array.

IX. CONCLUSION

A new approach for a broadband/multiband conformal circular beam-steering array is presented with essential theory and experimental data. The array consists of a center driven element with continuous 1.0–10 GHz bandwidth and broadband parasitic surface waveguide elements in the periphery for beam steering. It has an omnidirectional coverage with a medium antenna gain of 5–15 dBi, suitable for WLAN applications. Breadboard and brassboard development efforts for the array have achieved a bandwidth of 1.0–2.5 GHz except for two or three narrow bands of low performance. The functionality, physical compatibility, and low-cost feature of the array design have been well demonstrated.

The array is low-profile, suitable for mounting conformally on the top or bottom of a moving platform. Such broadband feature and low-profile conformability appear unattainable by conventional arrays. Perhaps more significant is its low production cost, which is estimated to be one order of magnitude lower than that of conventional beam-steering phased arrays.

At present, the ultra-wideband/multiband performance is limited only by the bandwidth of the surface waveguides. However, based on the successful broadbanding effort of the linear Yagi-Uda array with a bandwidth of $< 1\%$ at its inception to the 20:1 bandwidth achieved by the LP dipole array, the potential of unprecedented ultra-wideband and multiband performance, as well as an enormous low-cost advantage, for the present array is very promising. Therefore, its full broadband potential beyond 1-2.5 GHz, as well as performance enhancement within the 1-2.5 GHz band, is promising.

REFERENCES

- [1] H. Yagi, "Variable Directional Electric Wave Generating Device," U.S. Patent #1,860,123, May 24, 1932.
- [2] C. Sun, A. Hirata, T. Ohira, and N. Karmakar, "Fast beamforming of electronically steerable parasitic array radiator antennas: theory and experiment," *IEEE Trans. Antennas Propag.*, Vol. 52, No. 7, pp. 1819-1832, Jul. 2004.
- [3] J. J. H. Wang, "Broadband/Multiband Circular Array Antenna," U.S. patent pending, Mar. 29, 2004; U.S. provisional patent application filed Jun. 20, 2003; U.S. patent application filed Mar. 29, 2004.
- [4] J. J. H. Wang, D. J. Triplett, and C. J. Stevens, "Broadband/Multiband Conformal Circular Beam-Steering Array" *2005 IEEE MTT-S Int. Microwave Symp.*, Long Beach, CA, Jun. 2005.
- [5] J. J. H. Wang, "The Spiral as a Traveling Wave Structure for Broadband Antenna Applications," *Electromagnetics*, Vol. 20, No. 40, pp. 323-342, Jul-Aug 2000.
- [6] J. J. H. Wang, C. J. Stevens, and D. J. Triplett, "Ultrawideband Omnidirectional Conformable Low-Profile Mode-0 Spiral-Mode Microstrip (SMM) Antenna," *2005 IEEE AP-S Antennas Propag. Symp.*, Washington, DC, Jul. 2005.
- [7] J. J. H. Wang, "Broadband Miniaturized Slow-Wave Antenna," U.S. Patent #6,137,453, Oct. 24, 2000; Taiwan Patent #138,931, Jul. 21, 2001.
- [8] H. Jasik, editor, *Antenna Engineering Handbook*, 1st ed. New York, NY: McGraw-Hill, 1961.
- [9] R. C. Johnson, editor, *Antenna Engineering Handbook*, 3rd ed. New York, NY: McGraw-Hill, 1993.
- [10] Pistorius, "Theory of the Circular Diffraction Antenna," *Proc. IRE*, Vol. 36, No. 1, pp. 56-60, Jan. 1948.
- [11] J. J. H. Wang, *Generalized Moment Methods in Electromagnetics — Formulation and Computer Solution of Integral Equations*, New York, NY: Wiley, 1991, pp. 6-7, 105-107.
- [12] J. J. H. Wang, J. K. Tillery, G. T. Thompson, K. E. Bohannon, R. M. Najafabadi, and M. A. Acree, "A Multioctave-Band Photonicallly-Controlled, Low-Profile, Structurally-Embedded Phased Array with Integrated Frequency-Independent Phase-Shifter," *1996 IEEE Int. Symp. On Phased Array Sys. Tech.*, Boston, MA, Oct. 1996, pp. 68-73.



Johnson J. H. Wang (M'68-SM'79-F'92-LF'04) received a BSEE degree from National Taiwan University and a Ph.D. in electrical engineering from the Ohio State University in 1968.

Since 1991 he has been Chief Scientist and President of Wang Electro-Opto Corporation (WEO). From 1975 to January 1995, he was on the faculty of the Georgia Institute of Technology, Atlanta, Georgia. Prior to coming to Georgia Tech in 1975, he had seven years of industrial experience in the design of various antennas and phased arrays. At Georgia Tech his research was in the area of antennas, microwaves, and electromagnetic theory. A focus of his research was the computation of a variety of three-dimensional electromagnetic problems using digital computers by the method of moments. His current fields of interest are broadband/multiband low-profile conformable antennas and array antenna systems, multifunction and diversity antenna systems employing modern microwave and lightwave technologies, digital beam forming, as well as wireless telecommunications.

Dr. Wang is a Fellow of the Institute of Electrical and Electronics Engineers and a Member of The Electromagnetics Academy. He is the author of a book, *Generalized Moment Methods in Electromagnetics – Formulation and Computer Solution of Integral Equations*, John Wiley & Sons, New York, 1991.



David J. Triplett was born in Savannah, Georgia, USA on July 22, 1966. He received a B.S. degree in engineering from Georgia Institute of Technology in 1993.

During 1993-2000, his work was in the development and implementation of various computerized control systems, and modeling and simulation of processes (electromechanical, etc.) for a diverse range of applications. He joined Wang Electro-Opto Corporation (WEO), Marietta, Georgia in 2000 as an Engineer, and has since 2003 been a Senior Engineer. He has extensive experience in the integration of computer systems and their interface with other electrical and electromechanical systems, including both wired and wireless environments. Mr. Triplett also has extensive experience with a broad suite of programming languages, and their applications, gained over years since 1989. Since joining WEO in 2000, he has been actively engaged in antenna development, phased array systems simulation, and development of hardware and software for beam-steering arrays and smart antennas.



Christopher J. Stevens (M'04) was born in Massachusetts, USA on December 6, 1969. He received a B.S. degree in electrical engineering from the University of Massachusetts at Amherst, Massachusetts in 1996, specializing in microwave engineering and digital signal processing.

During 1988-1991 he was a Master Technician of the U.S. Air Force working on the ground electronics systems for the Minuteman III ICBM. Since 1996, he conducted various engineering and design work in the area of wireless telecommunications, with focus in antenna systems. He joined Wang Electro-Opto Corporation (WEO), Marietta, Georgia in 2002, and is now a Senior Engineer.

Mr. Stevens became a member of IEEE in 2004.